# Optimizing the density-matrix renormalization group method using quantum information entropy

Ö. Legeza[1,2] and J. Sólyom[1]
[1]*Research Institute for Solid State Physics, H-1525 Budapest, P.O. Box 49, Hungary*
[2]*Chair of Theoretical Chemistry, Friedrich-Alexander University, Erlangen-Nürnberg, D-91058 Erlangen, Egerlandstrasse 3, Germany*
(Received 15 May 2003; revised manuscript received 30 July 2003; published 21 November 2003)

In order to optimize the ordering of the lattice sites in the momentum space and quantum chemistry versions of the density-matrix renormalization group (DMRG) method we have studied the separability and entanglement of the target state for the one-dimensional Hubbard model and various molecules. By analyzing the behavior of von Neumann entropy we have found criteria that help to fasten convergence. An initialization procedure has been developed which maximizes the Kullback-Leibler entropy and extends the active space in a dynamical fashion. The dynamically extended active space procedure reduces significantly the effective system size during the first half-sweep and accelerates the speed of convergence of momentum space DMRG and quantum chemistry DMRG to a great extent. The effect of lattice site ordering on the number of block states to be kept during the RG procedure is also investigated.

DOI: 10.1103/PhysRevB.68.195116 PACS number(s): 75.10.Jm

## I. INTRODUCTION

The density-matrix renormalization-group (DMRG) method[1,2] has been widely used in recent years to study coupled fermionic and spin chain problems. Its application got a new momentum during the past few years when it was reformulated to models defined in momentum space[3] (MS-DMRG) or to quantum chemistry calculations[4,5] (QC-DMRG). The properties of the Hubbard model[6] and small diatomic molecules[7–10] have been studied using these methods. However, several new technical problems are raised by these versions of the DMRG that have to be solved to increase the efficiency of the method and to stabilize its performance.

A main difference between MS-DMRG and homogeneous lattice models studied by standard real-space DMRG with periodic boundary condition is that in the latter case each lattice site is equivalent and carries the same amount of information. In contrast to this, $k$ points or molecular orbitals lying closer to or further away from the Fermi surface have different information content. The method is very sensitive to the ordering of the $k$ points or molecular orbitals and an optimal ordering would have a major impact on the performance of MS-DMRG.[6,8–10] In fact the method can lose the target state and converge to a local minimum if an inappropriate ordering is used. It has also been found using the dynamical block state selection (DBSS) approach[9] that the same accuracy can be achieved with more or less block states, depending on the ordering.

The density matrices of composite systems, the separability of states, and the nature of entanglement have been extensively studied[11–19] in the past few years. Since MS-DMRG represents a composite system with long-range interactions the results of quantum information theory can be used to understand the criteria of convergence of MS-DMRG.

Another major feature that hindered the powerful application of MS-DMRG is the lack of the so-called infinite lattice method which in the real-space version generates a relatively accurate starting configuration for the so-called finite lattice method. In the initialization procedure proposed by Xiang[3] the environment blocks of various lengths were generated in advance of the finite lattice method. It is expected that a better procedure can be developed to generate the environment blocks by taking into account the change of the system block states during the process of renormalization. This is also crucial for reaching faster the crossover between the environment error and the truncation error. Then using the DBSS approach the accuracy is controlled by the threshold value of the truncation error fixed in advance of the calculations. The procedure relies on finding the most important states carrying the largest information. The space of these states will be called active space (AS) following a similar notation in quantum chemistry, namely, the CAS of the complete active space self-consistent field method used to define the orbitals for the configuration-interaction (CI) treatment. As it has been shown long ago[20] in the multireference configuration-interaction calculations the convergence depends not only on the size of the active space but on other constraints of the numerical treatment as well. It is, therefore, a very important task to develop a protocol that extends the active space more effectively.

From the point of view of synergetics DMRG can be interpreted as a dynamical system. In this analogy the response of a given model system to incident messages is studied and the change of the relative importance of messages is determined as the method converges to an attractor. Therefore, besides the practical importance to improve the MS-DMRG procedure, the study of the interaction of the subsystem blocks of DMRG as a function of the ordering of lattice sites is a very interesting question from the point of view of information theory, synergetics, and quantum data compression.[21–24]

Our aim in this paper is (1) to study the criteria of convergence of MS-DMRG by analyzing the structure of the superblock and subsystem density matrices and quantities used in quantum information theory, (2) to develop a more efficient initialization procedure that collects the most important block states required to describe the total system in a

 

better way, and (3) to study the effect of ordering on quantum data compression.

The setup of the paper is as follows. In Sec. II we describe the theoretical background of separability and entanglement, mutual entropy and relative importance of incident messages, and generation of information entropy. Numerical investigation of these quantities in the context of MS-DMRG and QC-DMRG is presented in Sec. III and optimization of ordering is shown in Sec. IV. Section V is devoted to the main steps of a protocol that uses a dynamically extended active space to improve the initialization procedure. It is shown how the Abelian point-group symmetry can be used in the framework of QC-DMRG. Numerical results obtained for the one-dimensional (1D) Hubbard model and for various molecules are presented in Sec. VI. and the effect of ordering on quantum compression is also analyzed in some detail. The summary of our conclusions and future prospectives are presented in Sec. VII.

## II. THEORETICAL BACKGROUND

### A. Separability versus entanglement

In general, if a finite system is divided into smaller subsystems (blocks) the Hamiltonian of the finite system is constructed from terms acting inside the blocks and the interaction terms among the blocks. The Hilbert space $\mathcal{G}$ of dimension $N$ of the system is formed from the direct product states of the subsystem basis states. In particular, if $\mathcal{G}$ describes a composite system with $m$ subsystems, then

$$\mathcal{G}=\otimes_{i=1}^{m}\mathcal{G}_i, \quad \dim \mathcal{G}=\prod_{l=1}^{m} N_l=N. \tag{1}$$

If $m=2$, then the system is called bipartite. In general, states of $\mathcal{G}$ can be pure states or mixed states described by the density matrix written as

$$\rho=\sum_i p_i|\psi_i\rangle\langle\psi_i|, \tag{2}$$

where $|\psi_i\rangle$ are eigenstates of the Hamiltonian acting on $\mathcal{G}$ and $\Sigma_i p_i=1$. The density matrix $\rho$ has the following properties: (i) $\mathrm{Tr}\rho=1$, (ii) $\rho$ is a positive operator, i.e., $\mathrm{Tr}(\rho P)\geqslant 0$ for any projector $P$, (iii) $\rho$ can be represented by its spectral decomposition as

$$\rho=\sum_{n=1}^{N}\alpha_n P_n, \quad \sum_{n=1}^{N}\alpha_n=1, \quad \alpha_n\geqslant 0, \tag{3}$$

where $P_n$ form a complete set of orthogonal projectors. A state $\rho$ is called separable if it can be written in the form

$$\rho=\sum_i p_i\otimes_{l=1}^{m}\rho_i^l, \tag{4}$$

where $\rho_i^l$ are states on $\mathcal{G}_l$, thus the subsystems are either not correlated or their correlation is purely classical.

In the density-matrix renormalization-group method proposed by White[1,2] the total system called the superblock has two sites $s_l$ and $s_r$ with $q_l$ and $q_r$ degrees of freedom between the left and right blocks $B_l$ and $B_r$ of dimensions $M_l$ and $M_r$, respectively. Thus the superblock can be considered as a specially constructed composite system. Its configuration is shown in Fig. 1.

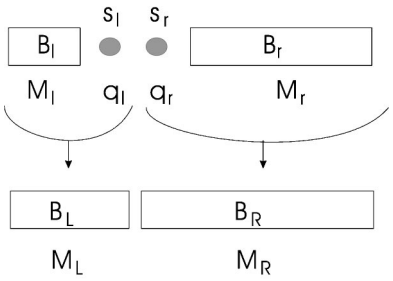


FIG. 1. Schematic plot of the system and environment block of DMRG. $B_l$ and $B_r$ denote the left and right blocks of lengths $l$ and $r$, and of dimensions $M_l$ and $M_r$, respectively, ● stands for the intermediate sites ($s_l$ and $s_r$) with $q_l$ and $q_r$ degrees of freedom. The blocks $B_L=B_l\bullet, B_R=\bullet B_r$ have dimensions $M_L$ and $M_R$, respectively.

The so-called target state ($|\Psi_T\rangle$) of the superblock system which is the eigenstate that one wants to calculate is formed from the direct product states of the blocks and the sites. It can be a coherent or incoherent superposition of several eigenstates. In the first case one deals with a pure state, while the latter corresponds to a mixed state. In this paper we examine only the first case, i.e., $|\Psi_T\rangle$ is chosen to be a pure state.

If we combine the $B_l\bullet$ composite system to one subsystem $B_L$ and $\bullet B_r$ to another one $B_R$, then the so-called superblock Hamiltonian for such a bipartite system consists of interaction terms determined in the blocks, denoted as $\mathcal{H}_L$ and $\mathcal{H}_R$ and interaction terms between the blocks denoted as $\mathcal{H}_{LR}$. The relative contribution of each term to the superblock energy can be measured as

$$\langle\mathcal{H}_i\rangle=\frac{\langle\Psi_T|\mathcal{H}_i|\Psi_T\rangle}{\left\langle\Psi_T\left|\sum_i \mathcal{H}_i\right|\Psi_T\right\rangle}, \tag{5}$$

where $i\equiv L,R,LR$ and $\Sigma_i\langle\mathcal{H}_i\rangle=1$.

Since the target state is a pure state it follows from the Schmidt decomposition that for $|\Psi_T\rangle\in\mathcal{G}=\mathcal{G}_L\otimes\mathcal{G}_R$, with $\dim\mathcal{G}_L=M_L$, $\dim\mathcal{G}_R=M_R$, $M_L\times M_R=N$,

$$|\Psi_T\rangle=\sum_{i=1}^{r\leqslant\min(M_L,M_R)}\omega_i|e_i\rangle\otimes|f_i\rangle, \tag{6}$$

where $|e_i\rangle\otimes|f_i\rangle$ form a biorthogonal basis $\langle e_i|e_j\rangle=\langle f_i|f_j\rangle=\delta_{ij}$, and $0\leqslant\omega_i\leqslant 1$ with the condition $\Sigma_i\omega_i^2=1$. If $r>1$ and in the range of a state $\rho$ there exists a $|\Psi\rangle$ such that

$$\Lambda=\langle\Psi|\rho^{-1}|\Psi\rangle^{-1}>\frac{1}{1+\max_{i\neq j}(\omega_i\omega_j)}, \tag{7}$$

or alternatively

$$\Lambda = \langle \Psi | \rho | \Psi \rangle > \max_i \omega_i^2, \tag{8}$$

then according to Ref. 14 $\rho$ is inseparable. If $\rho$ has an eigenvector $|\Psi\rangle$ corresponding to the eigenvalue $\Lambda$ such that the conditions in Eqs. (7) or (8) hold, then $\rho$ is inseparable. In our case for a pure state $|\Psi\rangle = |\Psi_T\rangle$ and $\Lambda = 1$. Using singular value decomposition to generate the Schmidt coefficients one can easily check if the conditions of Eqs. (7) or (8) hold or not for a given target state. The necessary conditions for a density matrix to be separable have been worked out by Peres[25] and Horodecki *et al.*[26]

Even if the target state is a pure state, the left or right blocks or the individual sites can be in a mixed state. A quantitative characterization of the degree of mixtures is provided by the von Neumann entropy. For a system with density matrix $\rho$

$$S(\rho) = -\mathrm{Tr}(\rho \ln \rho). \tag{9}$$

The von Neumann entropy is zero for a pure state and $S = \ln N$ for a totally mixed state with $\rho = (1/N)I$, where $I$ denotes the identity matrix of dimension $N$. Within the context of DMRG von Neumann entropies of the subsystems are calculated using the reduced density matrices given as $\rho_L = \mathrm{Tr}_R \rho$, $\rho_R = \mathrm{Tr}_L \rho$, $\rho_l = \mathrm{Tr}_{s_l} \mathrm{Tr}_R \rho$, $\rho_r = \mathrm{Tr}_L \mathrm{Tr}_{s_r} \rho$, $\rho_{s_l} = \mathrm{Tr}_l \mathrm{Tr}_R \rho$, $\rho_{s_r} = \mathrm{Tr}_L \mathrm{Tr}_r \rho$.

Alternatively, the so-called participation number

$$R(\rho) = \frac{1}{\mathrm{Tr}(\rho^2)} \tag{10}$$

can be used to characterize the mixture. The participation number varies from unity for pure states to $N$ to the totally mixed states and can be interpreted as an effective number of the states in the mixture. The Renyi entropy $S_q(\rho) = [\ln(\mathrm{Tr}\rho^q)]/(1-q)$ with $q > 1$ can also be used to measure how much a given state is mixed.

A fundamental concept related to inseparability and nonlocality of quantum mechanics is the entanglement. A typical example of the maximally entangled pure state for two spin-$\frac{1}{2}$ particles is

$$|\psi\rangle = \frac{1}{\sqrt{2}} |\uparrow\downarrow\rangle \pm |\downarrow\uparrow\rangle. \tag{11}$$

In order to measure the degree of entanglement between the blocks of DMRG one can make use of the entanglement monotone defined as $E: \rho(\mathcal{G}_L \otimes \mathcal{G}_R) \rightarrow R_+$ with (i) $E(\rho) = 0$ if $\rho$ is separable, (ii) $E$ is convex, and (iii) $E$ is nonincreasing (on average) under local quantum operations (quantum operations on the left or right block) or classical communications. A particular entanglement monotone, the entanglement of formation[27–29] is defined as

$$E_F(\rho) \equiv \min \sum_i p_i S(\mathrm{Tr}_R |\psi_i\rangle\langle\psi_i|), \tag{12}$$

where the minimum is taken over all the possible realizations of the state $\rho$, $\mathrm{Tr}_R$ is a partial trace with respect to the right block, $S$ is the von Neumann entropy defined in Eq. (9). For a pure state, Eq. (12) can be easily calculated. A mixed state is entangled if it cannot be represented as a mixture of factorizable pure states and there has been a great effort to determine a measure of entanglement for mixed states of a bipartite system.[29–31] In fact, according to Bennett *et al.*[27] all inseparable mixed states have nonzero ''entanglement of formation'' which means that a nonzero amount of pure entangled states are needed to build them.

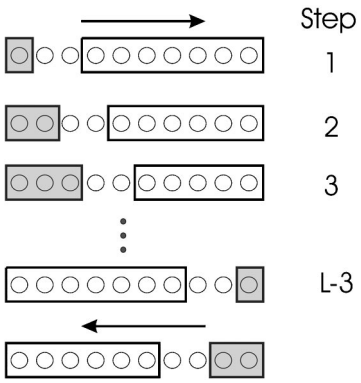


FIG. 2. The decomposition of the finite system to subsystems as a function of iteration steps corresponding to various partitionings. The shaded block represents the system block and the other block stands for the environment block. The arrows indicate the forward and backward sweeps.

### B. Mutual entropy and Kullback-Leibler entropy

In the DMRG procedure the complete Hilbert spaces of the blocks are truncated, thus they generate only a restricted subspace of the total Hilbert space. The various partitionings of the finite system containing $L$ lattice sites to subsystem blocks are obtained by systematically changing the sizes of the left and right blocks $(l)$ and $(r)$, respectively, with $l+2+r=L$ as shown in Fig. 2. In our implementation, described later in the text, the first iteration step corresponds to $l=1$ and $r=L-2-l$ and $l$ is increased as long as $l=L-3$. The renormalization procedure is used to obtain better configurations of the block states for a given partitioning yielding a more accurate description of the total system. In the forward sweep the left and right blocks are called the system and environment blocks, respectively. In the backward sweep the right block becomes the system block and the left block the environment block. In the DMRG method, the renormalized states of the system block are selected from the eigenstates of the reduced density matrix of the system block having the largest eigenvalues. The reduced density matrix is formed from the target state as $\rho_L = \mathrm{Tr}_R \rho$ and $\rho_R = \mathrm{Tr}_L \rho$ for the left and right subsystems, respectively, and $\rho = |\Psi_T\rangle\langle\Psi_T|$ is determined by the diagonalization of the superblock Hamiltonian. It is thus evident that since the various possible partitionings of the system have a strong effect on the structure of $\mathcal{H}_L, \mathcal{H}_R, \mathcal{H}_{LR}$ and on the density matrix of the superblock system, the structure of the reduced density matrix of the system block also depends on the environment block to a great extent. In this respect, states with largest eigenvalues of

the reduced density matrix of the system block can be considered as dominant states while states with smaller weights as recessive states. The term recessive is used to indicate that such a block state gives no considerable contribution to the superblock wave function with that given environment block, however, it is possible that it will provide a considerable contribution when it interacts with an environment block in a subsequent sweep of the finite lattice algorithm. The $M_{min}$ parameter introduced in Ref. 9 ensures that these recessive states are also carried on during the sweeping procedure until they might become a dominant state.

For a given system block various environment blocks can be constructed, and analogously to the genetic algorithm we can treat them as different species of a population with different information content. Alternatively, we can think of the environment blocks as sources of messages. A meaning can be attributed to a message if the response of the receiver, in our case the system block, is taken into account. Thus one can define the relative importance of message $\omega_j$ as the eigenvalues of the reduced density matrix. In other words, even if the environment block contains all the states of the restricted Hilbert space defined on the $r=L-l-2$ sites of the environment block, its information content can be very small if the system block is truncated so much that after taking into account the conservation of quantum numbers the Hilbert space of the total system (superblock) is reduced drastically. The opposite treatment when the system block is considered as the source of messages and the environment block as a receiver works in the same way. Therefore, one needs a protocol to measure the mutual information content of the blocks.

Before proceeding further we recall a few definitions from classical information theory in order to describe von Neumann entropy and its connection to quantum information theory. Let us assume that there are two events (not independent in general) described by two ensembles $(X^L,X^R)$ and two sets of probability distributions of the elements denoted as $p(x^L)$ and $p(x^R)$. We have used the labels $L$ and $R$ to indicate that the two events will later be related to the DMRG blocks. The Shannon entropy[32] for the two sets is defined as

$$S_i=-\sum_{j=1}^{M_i} p(x_j^i)\ln p(x_j^i), \quad \sum_j p(x_j^i)=1 \tag{13}$$

where $i\equiv L,R$. It is worth noting that the entropy depends only on the probability distribution $p(x_j^i)$. The largest uncertainty of an event corresponds to the uniform distribution with $p(x_j^i)=1/M_i$ where $M_i$ is the number of elements. If the state of the event is known exactly, then $S=0$ since $p(x_j^i)=1$ and all $p(x_{j'\neq j})=0$. Following the notation of Haken[33] Eq. (13) can be interpreted as an average of the quantity over $f_j$

$$S=\sum_j p(x_j)f_j, \tag{14}$$

where $f_j=-\ln p(x_j)$ and the weight is $p(x_j)$. In this respect $f_j$ is the information content of the state with index $j$ and $p(x_j)$ is the probability or relative frequency. If under a different condition we find a new relative frequency $p(x_j')$, then the change of information is

$$\Delta_j=\ln p(x_j')-\ln p(x_j). \tag{15}$$

To obtain the mean change of information, we average Eq. (15) over the new distribution function $p(x_j')$ and obtain the so called Kullback-Leibler information gain[34,35] as

$$K(p(x'),p(x))=\sum_j p(x_j')\Delta_j=\sum_j p(x_j')\ln\frac{p(x_j')}{p(x_j)}, \tag{16}$$

where $\Sigma_j p(x_j)=1$ and $\Sigma_j p(x_j')=1$. Equation (16) has an important property, namely,

$$K(p(x'),p(x))\geqslant 0. \tag{17}$$

If $X^L$ and $X^R$ are not independent of each other, then the so-called mutual information $I(L,R)$ quantifies the correlation between the two events, i.e., it gives the information about $X^L$ provided $X^R$ is known. $I(L,R)$ is written as

$$I(L,R)=S_L+S_R-S_{LR}, \tag{18}$$

where the total entropy $S_{LR}$ is calculated from the joint probability distribution of the two events $p(x_j^L,x_{j'}^R)$ as

$$S_{LR}=-\sum_{j,j'} p(x_j^L,x_{j'}^R)\ln p(x_j^L,x_{j'}^R). \tag{19}$$

It is clear from Eq. (18) that $I(L,R)$ is symmetric under the interchange of $X^L$ and $X^R$ and zero if and only if the two events are completely uncorrelated, i.e., when $p(x^L,x^R)=p(x^L)p(x^R)$.

The quantum analog of the Shannon entropy is the von Neumann entropy. In the context of DMRG it can be defined with $p(x_j^i)=\omega_j^i$, where $\omega_j^i$ are the eigenvalues of the reduced density matrices of the subsystems. The two events can be related to the left and right subsystem blocks. Since the target state was chosen to be a pure state it corresponds to zero von Neumann entropy with $S_{LR}=0$, thus $I(L,R)=S_L+S_R$. Recalling the Schmidt decomposition of Eq. (6) based on singular value decomposition one easily obtains that $\rho_L$ and $\rho_R$ have the same set of nonzero eigenvalues $(\omega_i=\omega_i^L=\omega_i^R)$ and

$$S_L=S_R=\sum_j \omega_j\ln\omega_j. \tag{20}$$

In what follows this will be denoted by $S$ and it is one half of the so-called mutual entropy. According to Eq. (12), $S$ is the measure of entanglement formation. In order to describe the relationship between entanglement and mutual entropy we can use Wootters's interpretation[28] obtained in quantum information theory. Within the context of DMRG it can be stated that for any pure target state the entanglement measures the amount of quantum information that must be exchanged between the DMRG blocks in order to create the target state.

For a given system block we can generate various environment blocks representing ''different conditions'' and the quantum analog of Eq. (16) called Kullback-Leibler entropy or quantum relative entropy is written as

$$K(\rho||\sigma) \equiv \mathrm{Tr}(\rho \ln \rho - \rho \ln \sigma), \tag{21}$$

where $\rho$ and $\sigma$ are two reduced density matrices of the system blocks corresponding to two different environment blocks.

In what follows $S$ is defined by Eq. (20) and $K$ by Eq. (21).

### C. Information generation and annihilation

In the above treatment a so-called static situation was considered where the DMRG system block has a given size with given lattice sites (orbitals) and we adjust the configuration space of the environment block. During the sweeping procedure of DMRG, however, the partitioning of lattice sites changes and the system behaves dynamically. In this case for a given incident message (given ordering and configuration space of the environment block) the algorithm drives the system to an attractor defined by the target state. As it has long been known, in a dynamical system, different incident messages can give rise to the same attractor, in which case one can speak of redundancy of messages. On the other hand, it is possible that one incident message can lead to two different attractors due to the fluctuation of the system or change of the intrinsic parameter of the system. This effect doubles the original information. As an example, it was found earlier[9] that if the symmetry of the target state was not restricted, then depending on the DMRG parameters the same ordering of lattice sites and initial conditions sometimes gave rise to the $S^z_{tot}=0$ component of the triplet state or to the singlet state. Clearly the relative importance of the message $\omega_j$ depends not only on the dynamical system but also on the tasks it must perform. In order to determine the values of $\omega_j$ of incident messages we have to consider the links between a message and the attractor into which the dynamical system is driven after receipt of this message. Following again the notation of Haken a single message can drive the system via fluctuations into several different attractors which may occur with branching ratios $M_{jk}$ with $\Sigma_k M_{jk}=1$. Then the relative importance $\omega_j$ is defined as

$$\omega_j = \sum_k L_{jk}\omega_k^{(1)} = \sum_k \frac{M_{jk}}{\sum_{j'} M_{j'k} + \epsilon}\omega_k^{(1)}, \tag{22}$$

where $\epsilon \to 0$. If there are several systems coupled one after the other, then for instance in a two-step procedure we obtain

$$\omega_j = \sum_k L_{jk}^{(1)}\omega_k^{(1)} = \sum_{k_1,k_2} L_{jk_1}^{(1)} L_{k_1k_2}^{(2)} \omega_{k_2}^{(2)}. \tag{23}$$

It is worth to emphasize that the recursion from $\omega^{(n)}$ to $\omega$ may depend on the path, namely, on the ordering of lattice sites or molecule orbitals. In such a way we obtain an interference of messages and the relative importance of messages depends on the messages previously delivered to the receiver. In the general case, the relative importance of a messages will depend in a noncommuting way on the sequence of the messages. In this way the receiver (in our case the system block) is transformed by messages again and again and clearly the relative importance of messages will be a function of the iteration step.

The meaning of Eq. (23) is that with a given task or ensemble of tasks, this algorithm allows us to select the message to be sent, namely, that with the biggest $\omega_j$. Using the relative importance of messages one can investigate the information entropy of subsequent states of the system,

$$S^{(0)} = -\sum_j \omega_j \ln \omega_j, \quad S^{(1)} = -\sum_k \omega_k \ln \omega_k, \tag{24}$$

whether a dynamical system annihilates, conserves, or generates information. If $\Sigma_k \omega_k = 1$ and $\Sigma_j \omega_j = 1$, there is annihilation of information if $S^{(1)} < S^{(0)}$ or generation of information if $S^{(1)} > S^{(0)}$. A dynamical system can be ''sensitive'' or ''insensitive'' for a given message. As it was described by Haken[33] it is an interesting problem to determine the minimum number of bits required to realize a given attractor or to realize a given value of ''relative importance.'' The $M_{min}$ parameter introduced in a previous work[9] had the same meaning. It is, however, a major task to determine those incident messages that have the largest $\omega_j$ in advance of the calculations.

## III. NUMERICAL INVESTIGATION OF von NEUMANN ENTROPY AND ENTANGLEMENT

The elements of information theory outlined in the previous sections have been used in the DMRG studies of systems described by the Hamiltonian

$$\mathcal{H} = \sum_{ij\sigma} T_{ij} c_{i\sigma}^\dagger c_{j\sigma} + \sum_{ijkl\sigma\sigma'} V_{ijkl} c_{i\sigma}^\dagger c_{j\sigma'}^\dagger c_{k\sigma'} c_{l\sigma}, \tag{25}$$

where $T_{ij}$ denotes the matrix elements of the one-particle Hamiltonian and $V_{ijkl}$ stands for the matrix elements of the electron interaction operator. Depending on the structure of $T_{ij}$ and $V_{ijkl}$ this Hamiltonian can describe a molecule or a usual fermionic model in solid-state physics, e.g., the Hubbard or extended Hubbard models in one or higher dimensions or, for example, coupled fermion chains. In the former case a one-dimensional chain is built up from the molecular orbitals that were obtained, e.g., in a suitable mean-field or MCSCF calculation and in the rest of the paper we use the numbering of orbitals corresponding to the output of these calculations. In our solid-state physics applications the indices $i,j,k,l$ denote momenta with $k_i = (2\pi n)/L, -L/2 < n \leq L/2$. For the one-dimensional Hubbard model $T_{ij} = -2t\cos(k_i)\delta(i-j)$ and $V_{ijkl} = (U/L)\,\delta(i+j-k-l)$. In what follows $U$ is given in units of $t$ with $t=1$. In the rest of the paper Hartree-Fock (HF) orbitals denote filled $k_i$ points between the Fermi surfaces ($\pm k_F$) in the limit of $V_{ijkl}=0$ where we use ''Fermi surface'' to denote sites where the occupation number of the sites drops to zeros for $V_{ijkl}=0$. The full CI (FCI) energy is the exact solution of Eq. (25) for

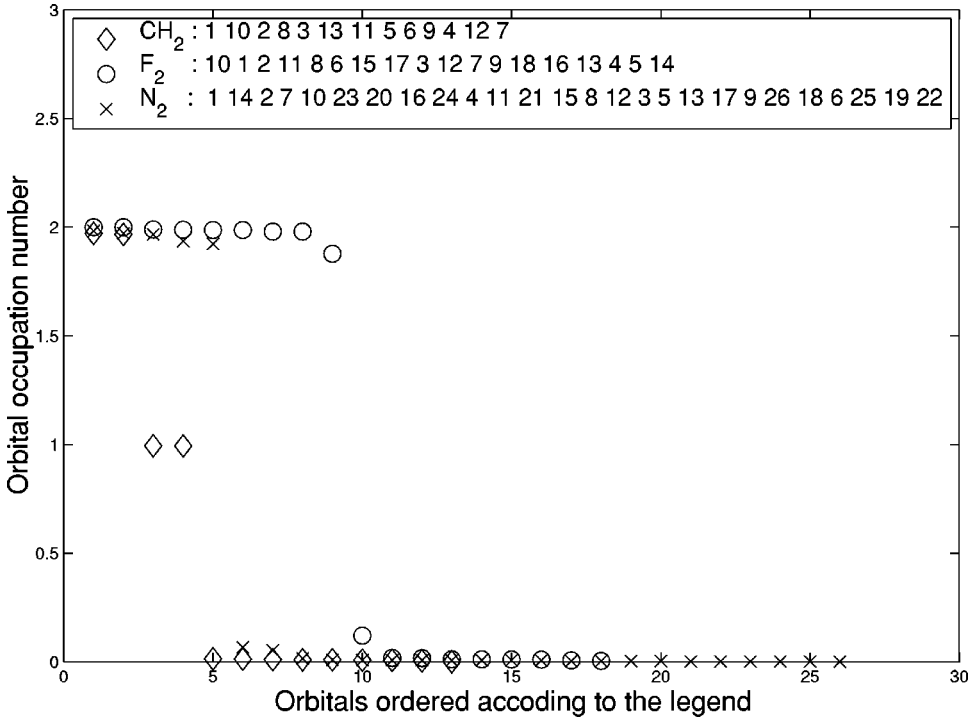


FIG. 3. Decay of orbital occupation number obtained in the full CI limit and the corresponding ordering of orbitals for the molecules studied in the paper.

a finite chain with length $L$ and for a given number of electrons with up and down spins. The relative error of the energy is written as

$$E_{rel}=\frac{E_{\mathrm{DMRG}}-E_{\mathrm{FCI}}}{E_{\mathrm{FCI}}}. \tag{26}$$

In our DMRG calculations we have used the DBSS approach in which case the number of block states is selected dynamically according to the threshold value of the truncation error $\mathrm{TRE}_{max}$ set up in advance of the calculations. The other free parameters $M_{min}$ and $M_{max}$ control the minimum and maximum number of block states to be kept during the renormalization procedure, respectively. We have often used different values of $M_{min}$ for the blocks, thus in what follows $M_l^{min}$ and $M_r^{min}$ stand for the left and right blocks, respectively.

### A. Analysis on small molecules

First we have analyzed the density matrices and the energy of the subsystem blocks and the interaction between the subsystem blocks by carrying out test calculations on a very small system, namely, the $CH_2$ molecule by correlating 6 electrons on 13 orbitals. The system is so small that it is hardly expected that DMRG would not converge to the attractor determined by the target state. In the ordering we relied on the occupation number of the orbitals obtained in the full CI calculation by the MOLPRO program package.[36] This is plotted in Fig. 3 for a few selected test molecules used in the present paper. The legend shows the corresponding orbitals with the original indices. It is worth mentioning that for the $CH_2$ molecule orbitals 1 and 10 are almost doubly occupied while orbitals 2 and 8 are almost occupied with up or down spins since the ground state is a triplet state.

In a first attempt to generate a good environment block, we have put the orbitals with the largest occupation numbers to the right end of the chain. This corresponds to the following ordering: [7,12,4,9,6,5,11,13,3,8,2,10,1]. Our result obtained for a truncation error $\mathrm{TRE}_{max}=10^{-8}$ is shown in Fig. 4. In the subsequent panels we show the number of selected block states, the relative error of the energy, the relative energy of the blocks and the interaction term, the mutual entropy, the site and block entropies, and the site participation numbers as a function of DMRG iteration step. The number of iteration steps when the half-sweep ends are at 10,19,28,37. It is evident from the figure that although depending on $\mathrm{TRE}_{max}$ the number of selected block states fluctuated, the energy did not converge to the FCI value. It was trapped at some local minimum. This extreme situation has often been found in our previous studies. Investigating the third panel of the figure, it is obvious that the right block alone provides all the contribution to the superblock Hamiltonian as ($\langle H_R\rangle \simeq 1$) and the interaction between the blocks vanishes ($\langle H_{LR}\rangle \simeq 0$), except at the turning points. Due to the lack of interaction of the blocks the mutual information entropy of the blocks remained close to zero, thus no quantum information exchange was generated during the sweeping procedure as can be seen on the fourth panel of the figure. In order to analyze the information content of the subsystems we have also plotted in the fifth panel the calculated entropies of the left and right blocks ($S_l$ and $S_r$) and the entropies of the two intermediate sites ($S_{s_l}$ and $S_{s_r}$). The sixth panel shows the participation numbers of the two intermediate sites ($R_{s_l}$ and $R_{s_r}$). It is clearly seen that sites lying close to the Fermi surface have much larger von Neumann entropy ($S_{s_l}$,$S_{s_r}$) and larger participation number ($R_{s_l}$,$R_{s_r}$) than orbitals where the occupation number is close to zero or

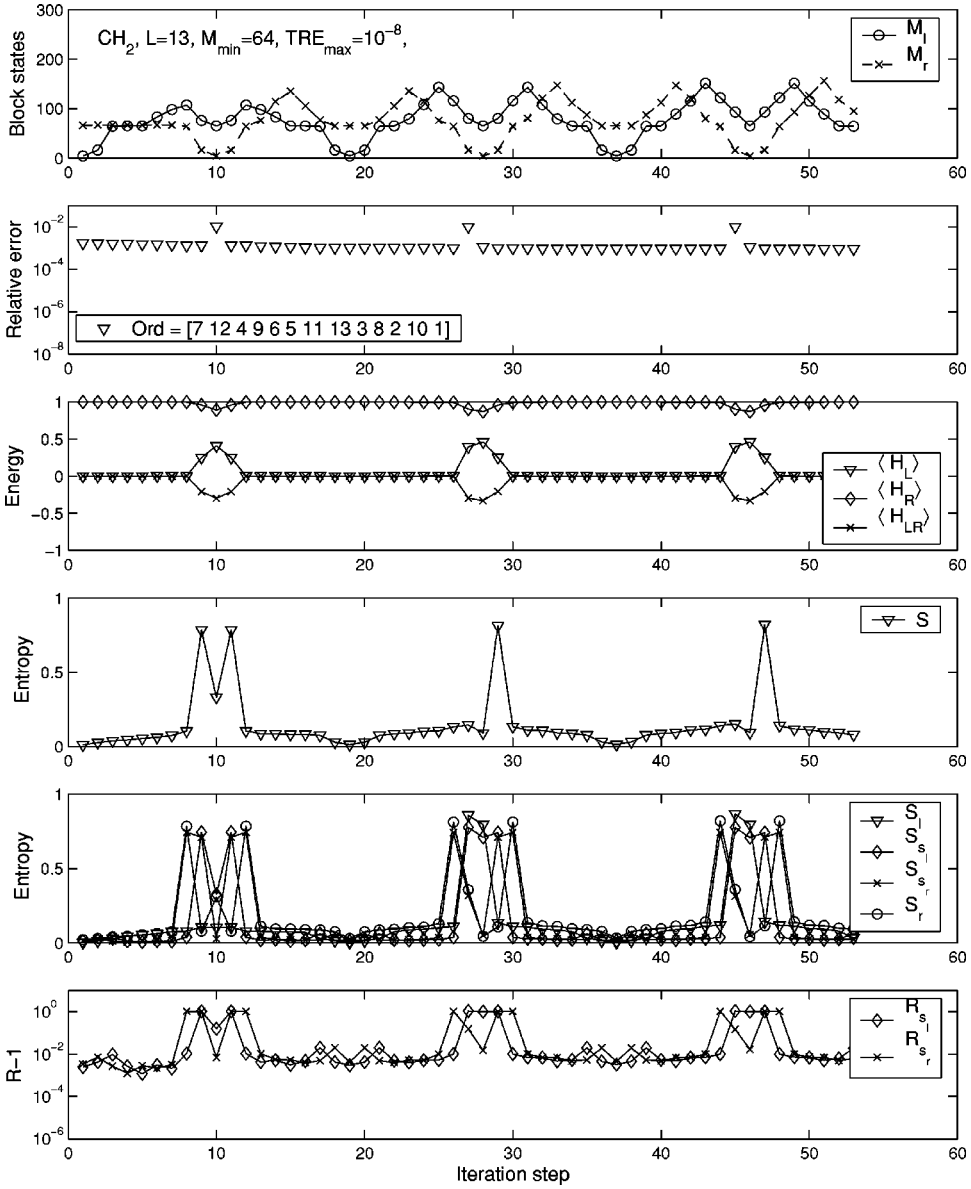


FIG. 4. Example for an ordering when relevant information of the system is collected into one DMRG block giving rise to vanishing interblock interactions and very low entropy indicating high separability of the target state and lack of quantum information exchange between the blocks.

2. (This is determined by identifying the data points corresponding to the ordering and the partitioning of the composite system for that given iteration step as was shown in Fig. 2.) The meaning of site entropy and participation number can be explained very easily. In our case in the four-dimensional basis states $(0,\uparrow,\downarrow,\uparrow\downarrow)$ the maximally mixed state would correspond to $S=\ln 4$ and $R=4$. For those sites which lie energetically far above ( below) the Fermi surface the $|0\rangle$ $(|\uparrow\downarrow\rangle)$ basis state in the reduced density matrix of the site would appear with very large probability and the remaining three basis states with vanishing probability giving rise to $S\simeq 0$ and $R\simeq 1$. In contrast to this, the reduced density matrices of sites lying close to the Fermi surface will have a more uniform eigenvalue spectrum corresponding to a finite value of the entropy and a participation number larger than unity. Analyzing the situation close to the turning points, we have to recall that in this case the $\bullet B_r$ subsystem contains two lattice sites, but orbitals 1,10,2,8 are very important components of the wave function. Therefore, both subsystems contain important states and a finite quantum information exchange between the blocks is necessary in order to generate the target state. As a test we have flipped the ordering and found a similar behavior, except that the peaks of the interaction terms and the entropies were shifted to the other end of the chain.

As a next step, the interaction between the blocks was maximized by putting the orbitals alternatively to the two ends with decreasing occupation number. This gives the following ordering: [1,2,3,11,6,4,7,12,9,5,13,8,10]. Our result is shown in Fig. 5. It can be seen that the convergence became very fast and within one and a half sweeps (26 iterations steps) the error margin set by $\mathrm{TRE}_{max}$ was reached. This means that the environment error was reduced significantly within one full sweep. Investigating the third panel one can see that there is always a strong interaction between the blocks as $\langle \mathcal{H}_{LR}\rangle \simeq -0.5$ and both blocks provide equal amount of energy for the total system as $\langle \mathcal{H}_L\rangle \simeq \langle \mathcal{H}_R\rangle \simeq 0.7$. Analyzing the separability and entanglement of the

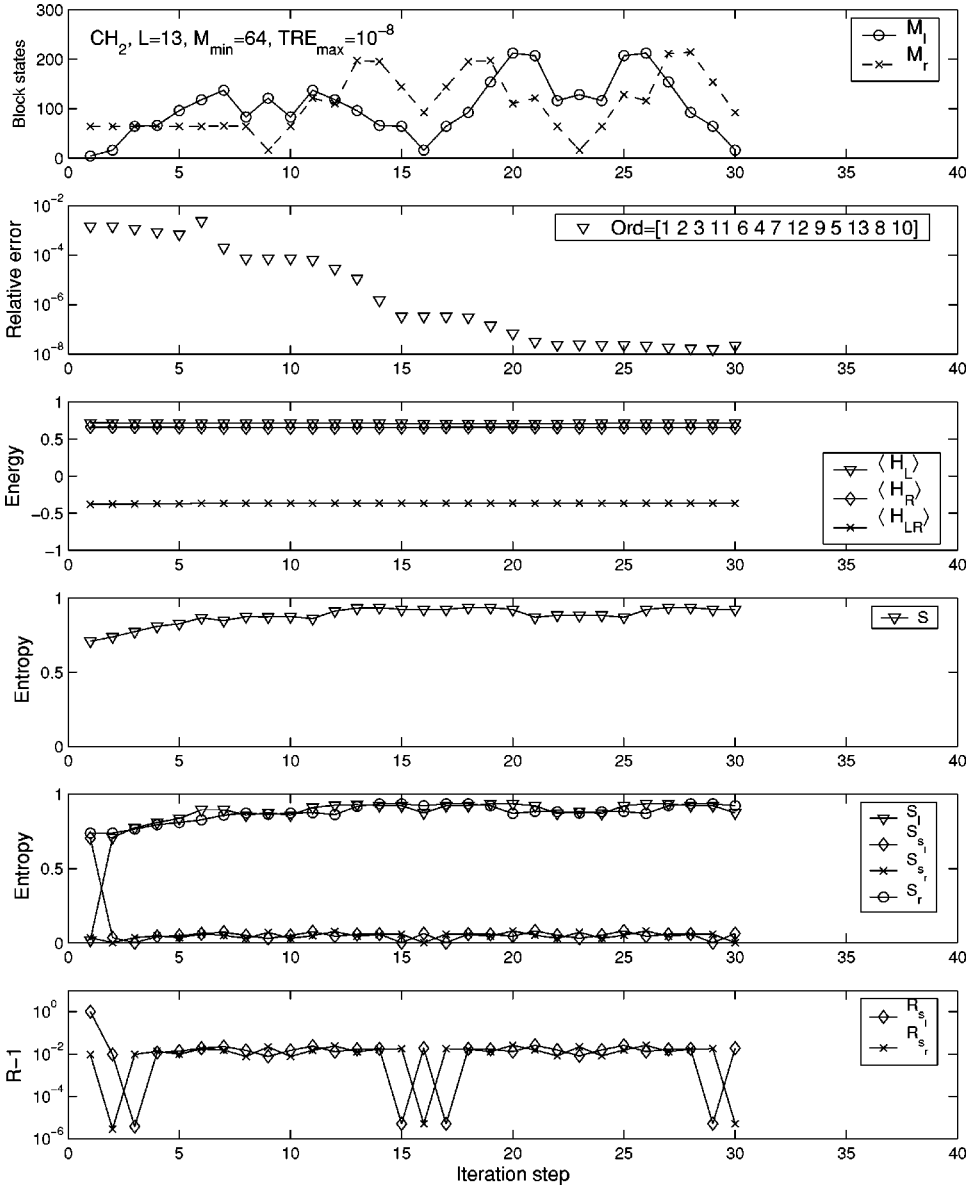


FIG. 5. Same as Fig. 4 but for an ordering when relevant information of the system is shared between DMRG blocks giving rise to strong interblock interaction and large quantum information exchange between the blocks.

target state the fourth panel shows that the system possesses large mutual entropy indicating a large entanglement and a large amount of quantum information exchange between the blocks. Another major difference compared to the results obtained for the previous ordering is that the block entropies ($S_l$ and $S_r$) are always very large as can be seen in the fifth panel.

Investigating the first panel of Fig. 5 one can see that the maximum number of block states selected dynamically were often close to 250. Based on previous studies we expect that the Cuthill-McKee algorithm[37] gives a better ordering in the sense that a smaller number of block states have to be selected to achieve the same accuracy. Our result for the ordering [7,6,5,4,3,1,2,9,8,13,12,10,11] is shown in Fig. 6. It can be seen that in fact the same accuracy was achieved as before with a smaller subset of block states [$\max(M)<130$]. At the same time the mutual entropy had usually large peaks when the energy improved significantly. Analyzing the fifth and sixth panels one sees that orbitals which have large entropy are now at the center of the chain and the site entropies had maxima where the mutual entropy had sharp peaks. In addition, compared to the two previous orderings it is evident that the minimum of $R$ was at larger values. Looking at the third and the fourth panel we can find an extended region with large interblock couplings but with small entropy. For this region our result seems to indicate smaller entanglement between the blocks, thus it might correspond to a more pronounced finite classical interblock interaction with less quantum correlation between the blocks. Again the significant improvement in the energy happens when the two blocks have the same amount of intrablock energy with a large quantum information exchange between the blocks.

### B. Analysis on larger molecules

In order to search for an optimal ordering method we studied the quantities defined above for the molecules $CH_2$, $H_2O$, $F_2$, and $N_2$. We have found that in general the Cuthill-

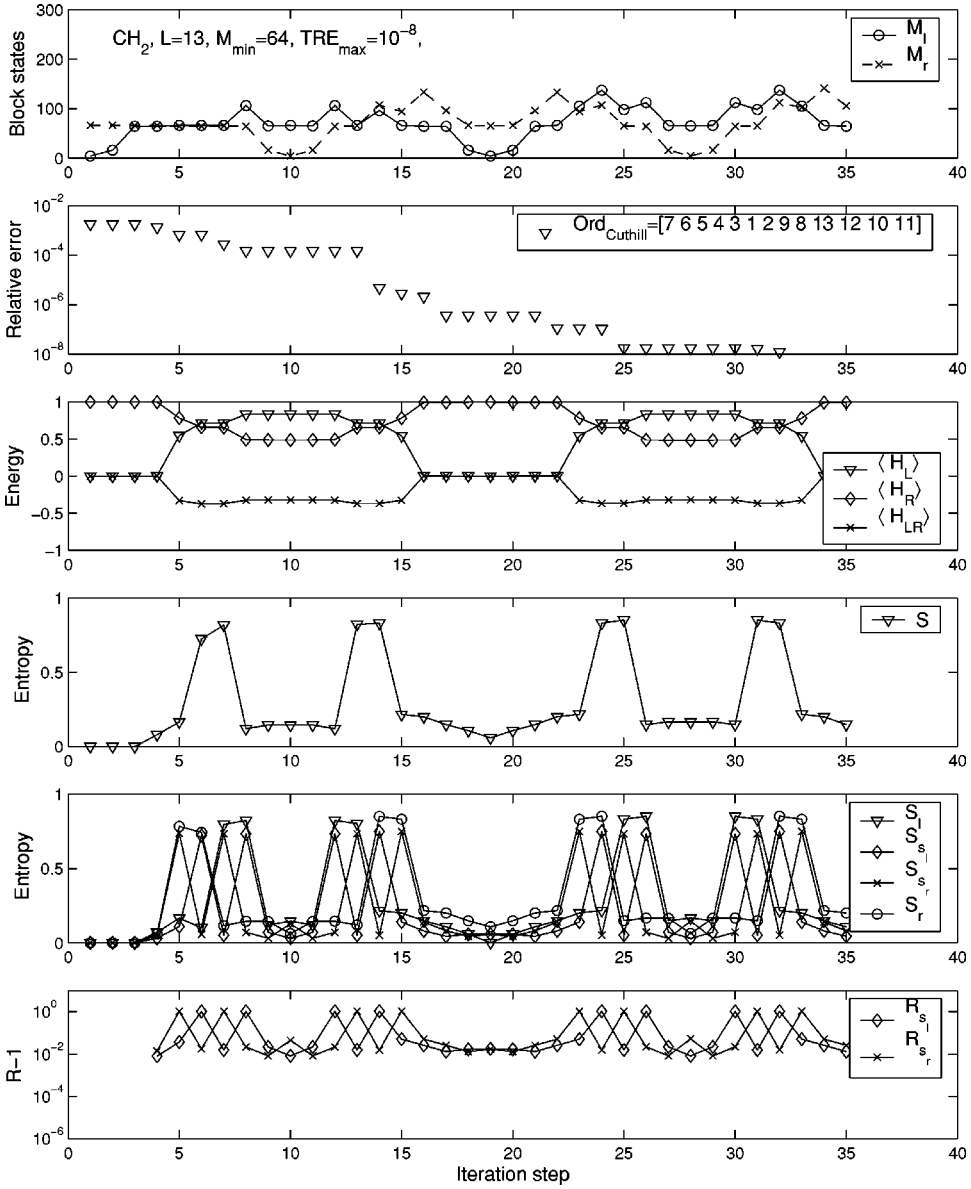


FIG. 6. Same as Figs. 4 and 5 but for the Cuthill-McKee ordering.

McKee ordering is not the best one. In the case of $F_2$ molecule with 18 electrons on 18 orbitals DMRG did not converge at all, as can be seen in Fig. 7. The number of iteration steps when the half-sweep ends are at 15,28,41,54. It is evident from the figure that the orbitals with larger participation number and larger entropy appear close to the two ends of the chain and the method performed rather badly. A large number of block states were selected (we have cut $M_{max}$ at 2000) and the result did not converge. Cuthill-McKee ordering resulted in a very similar distribution of site entropies as in the second example for the $CH_2$ molecule. We have tested this kind of entropy distribution for the other molecules as well using larger basis sets and obtained very slow convergence or lack of convergence. Therefore, the good convergence obtained in the second example for $CH_2$ molecule was due to the short chain length.

### C. Analysis on the 1D Hubbard chain

We have done similar calculations on the 1D Hubbard model for various band fillings, chain lengths, and $U$ values. Figure 8 shows six different orderings of the $k$ values for a half-filled $L=14$ chain. The first panel corresponds to the natural ordering, where the values $-\pi<k_i\leqslant\pi$ follow each other with increasing $k_i$, the doubly filled states of the HF state are on the sites 4,5,6,7,8,9,10, the others are empty. The states at the Fermi energy are on the sites 4,10. In the second panel the ordering of sites with negative and positive momenta was reversed. In the third panel sites counted from the Fermi surface were ordered to one side of the chain similarly to the first example used for $CH_2$. In the fourth ordering the Fermi points were moved to the two ends of the chain similarly to the second example used for $CH_2$. The fifth and sixth panels show our attempts to place the sites near the Fermi surface to the center of the chain as in the third example for the $CH_2$ molecule.

We have found similar results as for the molecules, namely, the third ordering gave the worst result. For small $U$ values ($U\simeq 0.5,1$) the method did not converge even if $M_{min}=800$ was used. The fourth ordering gave very large

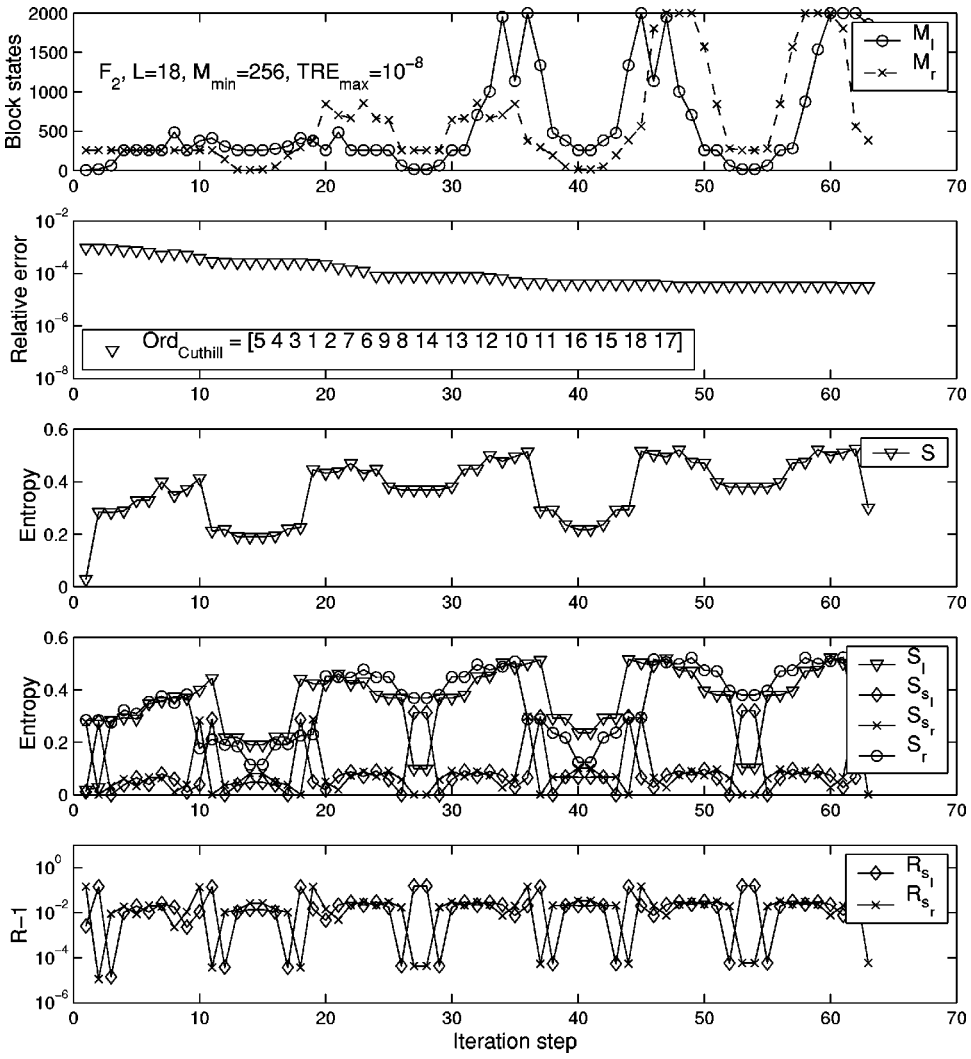


FIG. 7. Result for $F_2$ molecule correlating 18 electrons on 18 orbitals using Cuthill-McKee ordering.

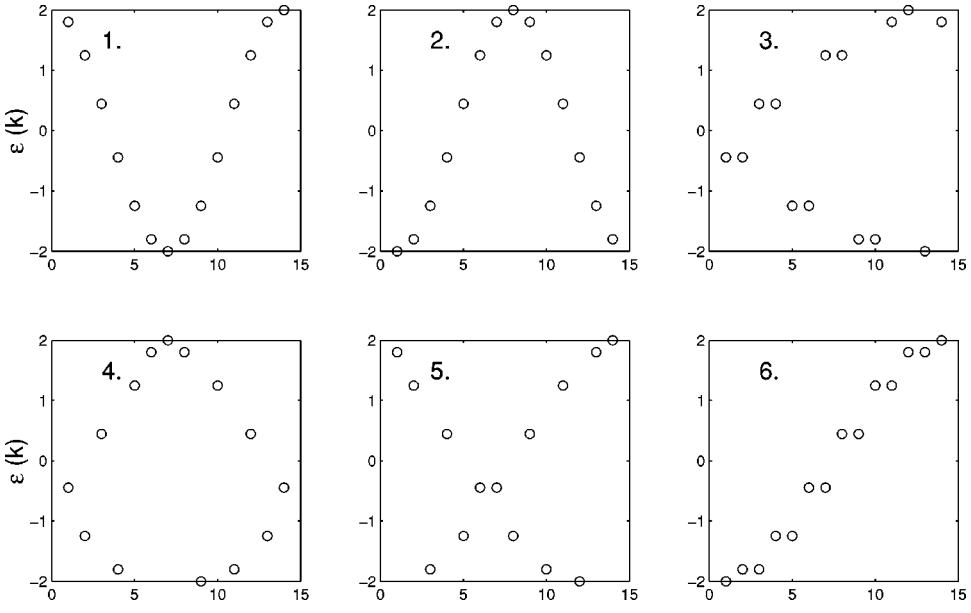


FIG. 8. Examples for various orderings of $k_i$ points for the half-filled Hubbard chain with $L=14$. Doubly filled sites in the HF limit in the natural ordering are 4,5,6,7,8,9,10.

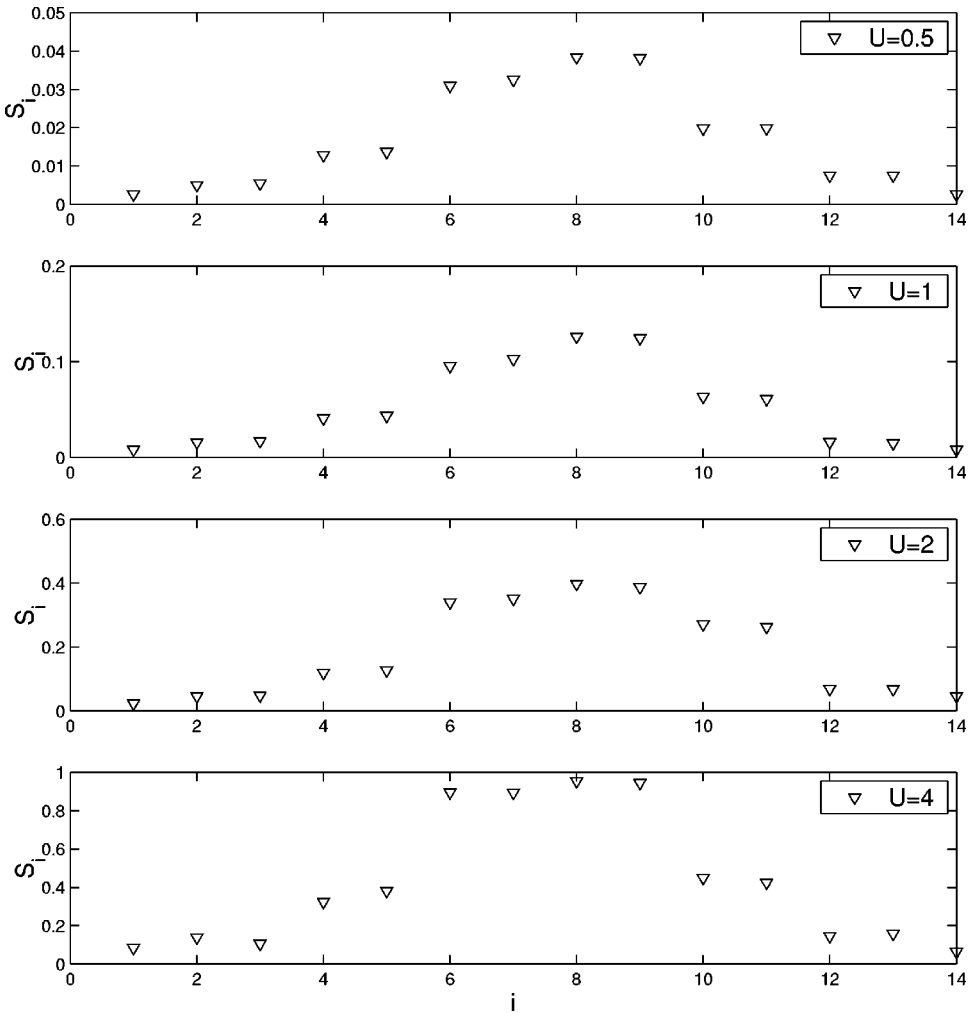


FIG. 9. Site entropy $S_i$ obtained for the half-filled Hubbard chain with $L=14$ using ordering shown on the sixth panel with $U=0.5,1,2,4$.

mutual entropy in almost all iteration steps and although a very large subset of block states was selected, the convergence was still very slow. It required six to seven sweeps for a half-filled chain with $L=14$, $U=1$, and $\mathrm{TRE}_{max}=10^{-6}$. The best performance was obtained for the fifth and sixth orderings. The first two orderings gave stable but considerably slower convergence.

We have carried out several calculations with chain lengths up to 30 sites for various fillings and $U$ values and found again that good convergence is obtained if the block entropies are not very small for several iteration steps whose values depend on the various model parameters. As an example the distribution of site entropy for the half-filled Hubbard model with $L=14$ using the sixth ordering is shown in Fig. 9. Data points have been taken from $S_{s_l}$ and $S_{s_r}$ by carrying out an additional full sweep after the DMRG method has converged. As can be seen, larger $U$ values gave larger values of site entropies which means more mixed states. In addition, for increasing $U$ values, where sites lying further away from the Fermi surface become more important, we have found that DMRG blocks had finite interaction strength for all iteration steps but, of course, the number of maximally selected block states has increased significantly. As an indication for an $L=14$ half-filled chain a $10^{-5}$ absolute error of the energy has been reached with max($M$) $\simeq$400–500 for $U=0.5$, while the system selected out dynamically more than 2000–2500 states to reach an accuracy of $10^{-4}$ for $U=4$. For $L=18$ these numbers are 600–700 and 3000–3500, respectively. This fact questions the efficiency of MS-DMRG when $U$ is comparable to or larger than the band width. We expect that for the large $U$ limit real-space DMRG should provide more accurate results.

We have also found that the best ordering is a function of the filling. This is because the algorithm will converge only if there is a finite interaction between the blocks for several iteration steps, and therefore both blocks must contain sites with large entropies. For half-filling the best ordering is that shown on the sixth panel in Fig. 8. For lower filling, however, this ordering can lead to a situation shown in the first example for the $CH_2$ molecule. As an example for the 6/18 Hubbard chain for $U=0.5$ the ordering scheme of panel 6 in Fig. 8 leading to [9,8,10,7,11,6,12,5,13,4,14,3,15,2,16,1,17,18] the DMRG method is trapped by a local attractor since for several steps one block contains all the important sites and there is no interaction between the blocks. If sites with large entropies are placed at the center of the chain as in the natural ordering or for the ordering [2,1,4,3,6,5,8,7,9,11,10,13,12,15,14,17,16,18], the DMRG method converged to the desired accuracy within two sweeps. The

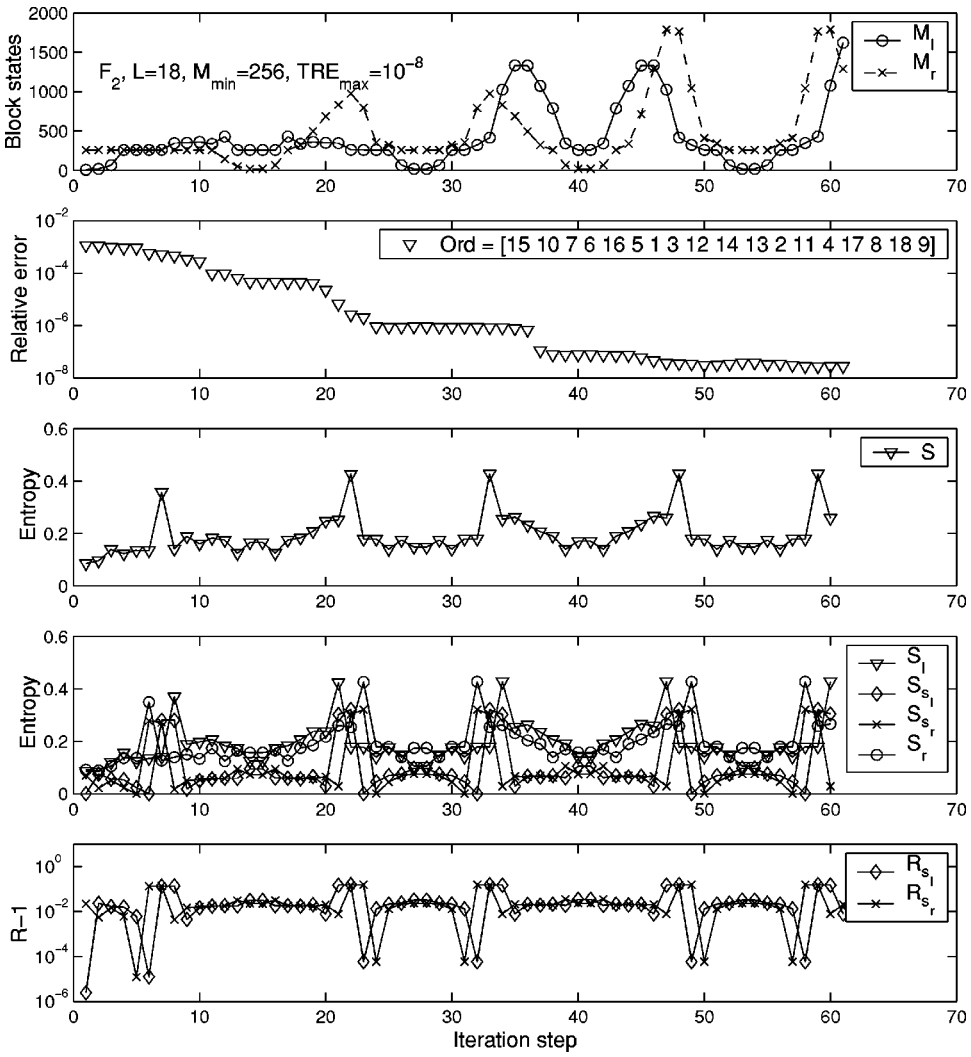


FIG. 10. Result for $F_2$ molecule correlating 18 electrons on 18 orbitals using our numerically optimized ordering.

last two orderings also lead to the reduction of block entropies and the number of selected block states for several iteration steps.

We can thus conclude that DMRG converges only if the block entropies and mutual entropies are not very small, but at the same time it is not a good strategy to choose an ordering with which the entropy is large for all iteration steps. There is an optimal configuration in which case the block entropies are large for several iteration steps but small otherwise. This can be achieved by moving sites with largest entropies close to each other and closer to the center of the chain.

## IV. OPTIMIZING ORDERING

It is very important to emphasize that according to Eq. (23) the dynamics of the system depends very much on the path it evolves, thus on the way it receives incident messages and the renormalized block states are formed. In DMRG the initial wave function does not point in the direction of the attractor and it is rotated systematically in the multidimensional space by the transformation matrices during each renormalization step. The sequence of rotation, however, is not commuting, therefore, as it has been seen in the calculations presented above, the ordering has a great impact on the structure of renormalized states. For fermionic models the optimal ordering following from our earlier considerations is a function of the filling and $U$ value and is obtained if sites with large entropies are placed close to each other at the center of the chain.

It is a far more complicated task to find the optimal ordering in quantum chemistry. In order to search for an optimal ordering we have carried out a kind of brute force calculation for the $F_2$ molecule. We have run QC-DMRG using 64 block states for one half-sweep, then permuted two orbitals and monitored the obtained energy values. If an ordering produced a better result, it was kept and a next ordering was obtained by permuting again two sites. For the $F_2$ molecule one calculation took some 8 s CPU time and more than 50 000 permutations were carried out. Our result for the best ordering is shown in Fig. 10. It can be seen that the sites with largest entropy are close to the center of the chain but some sites with finite entropy are close to the two ends of the chain. This configuration is in agreement with what has been found for the Hubbard chain. It provides finite interaction between the blocks for several steps but the largest information exchange between the blocks occurs when the super-

block composite system is close to a symmetric configuration. We have investigated the other test molecules as well and obtained similar results. It is worth mentioning that for a given molecule the ordering that produced the best performance at the end of the first half-sweep also gave the fastest convergence using more sweeps.

As a summary of our result, we have obtained the following rule to generate a good ordering, which, of course, could still be not the optimal one.

*Step 1*. The Cuthill-McKee ordering is used and a DMRG calculation with some 100 block states is run and the entropies, participation numbers, and orbital occupation numbers are determined.

*Step 2*. The orbitals with largest entropies (largest participation numbers, closest to the Fermi surface) are moved to the center of the chain and the remaining orbitals are distributed along the chain with decreasing entropies counted from the two ends of the chain.

This method guarantees a finite interblock coupling for several steps but reduces the number of block states. It is worth mentioning that if $q^r \leqslant M_r^{min}$ or $q^l \leqslant M_l^{min}$ then the sweeping procedure can be turned back, since the remaining part of the sweeping will not improve the environment. All calculations in the rest of the paper were obtained following this rule.

## V. THE INITIALIZATION PROCEDURE

Besides ordering, the optimal performance of DMRG is strongly effected by the initial conditions or in other words by the initial block configurations. Looking at Fig. 6 one can see that in the first three iteration steps the mutual entropy $S$ was exactly zero, $R_{s_l}$ and $R_{s_r}$ was unity $(R-1=0)$ while in the second sweep at the same partitioning their values became larger indicating a better environment block. In addition, for the first three iteration steps the eigenvalue spectrum of the reduced density matrix of the system block $(\rho_L)$ had one eigenvalue of unity which according to Eq. (8) means that the superblock eigenstate was separable. For the second sweep all eigenvalues were less than unity indicating that the target state became nonseparable. Since the subsystem entropies and related quantities depend on other subsystems, this suggests that a better initialization procedure can be obtained if one starts with a larger mixture by increasing the block entropies. This also leads to the decrease of the volume of separable basis states of the target state. We have also found that the entropy of the blocks must be larger than a critical value.

The standard initialization procedure outlined by Xiang, when subsystem blocks of various lengths (describing various partitions) are generated in advance of the finite lattice algorithm, does not guarantee this in general for the first sweep. Therefore, it is crucial to develop a method that constructs the environment blocks by taking into account the change of the renormalized system block basis states, and which increases the block entropies above a threshold value during the initialization procedure. In this section we present a procedure to generate the system and environment blocks giving large $\omega_j$ eigenvalues, i.e., block entropies.

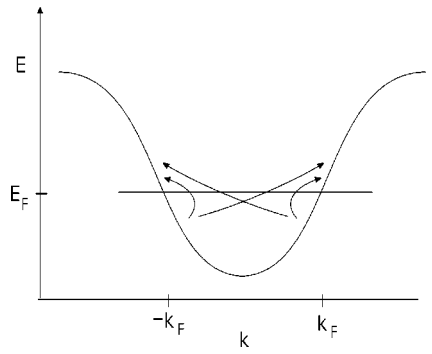


FIG. 11. Dispersion relation of the 1D Hubbard chain. Arrows indicate the most probable electron-hole excitations with small momentum transfer in the small $U$ limit.

### A. The dynamically extended active space procedure

Let us consider first the partitioning where the left block (system block) contains one lattice site and the right block (environment) $L-3$ lattice sites as was shown in Fig. 2. The system block contains $M_l=q$ states and the right block contains $M_r$ states when the conservation laws of total quantum numbers are taken into account. The various configurations of the right block interact differently with the left block. Since the density matrix of the system block depends strongly on the interaction between the two blocks the initial configurations of the right block have a strong effect on the renormalized block states of the left block. In order to guarantee the convergence of DMRG the mutual entropy should possess a finite value, thus one needs a method that maximizes the Kullback-Leibler entropy given by Eq. (21), i.e., a protocol to optimize the right block configuration in advance of the calculation to have largest von Neumann entropy.

It is known for the Hubbard model that for small $U$ all the interesting physical properties are determined by sites that lie close to the $\pm k_F$ Fermi points. They give also the largest contribution to the correlation energy. The most important excitations are shown in Fig. 11. As the strength of $U$ is increased, this region gets larger and sites further away from the Fermi points will also contribute to the correlation energy and other physical properties. We can thus expect that the basis states formed from the sites around $\pm k_F$ will correspond to a larger mixture (several $\omega_j$ will be large) and we can form the incident message from these states. In order to achieve this we define a so-called AS vector, a concept inherited from quantum chemistry which simply contains the most important sites in a descending order with respect to their expected importance. For the Hubbard chain this vector is $AS \equiv [k_F, -k_F, k_F+1, -k_F-1, k_F-1, -k_F+1, \ldots]$. In QC-DMRG the AS vector is constructed in a self-consistent way. First the AS vector is defined to include only the HF orbitals and a quick calculation is performed with some 100 block states using one or two sweeps. Next the AS vector is defined by taking orbitals with largest values of site entropies in a descending order.

We have confirmed numerically that the entropy of the environment block $(S_r)$ can be increased by using sites lying around the Fermi points. Once a good AS vector is established, the question arises how to construct the configuration

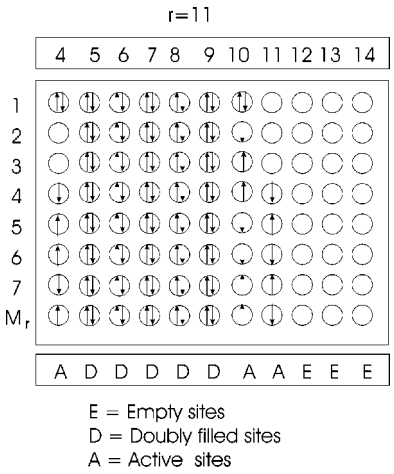


FIG. 12. Example for a right block configuration space obtained by the DEAS procedure for the half-filled Hubbard chain with $L=14$, $N_{\uparrow}=N_{\downarrow}=7$, $M_r^{min}=8$, $l=1$, $r=11$ and HF vector $\equiv[4,5,6,7,8,9,10]$ and AS vector $\equiv[4,10,3,11,5,9]$. The numbers in the first row label the site indices along the chain.

space, i.e., how to fill the sites given by the elements of the AS vector? Therefore, one needs a protocol that extends optimally the active space in order to achieve fast convergence. In the following we describe the details of the dynamically extended active space (DEAS) procedure which takes into account the change of the partitioning of the DMRG superblock and the renormalization procedure of the system block.

Let us assume that we have a given ordering and we have a starting partitioning with $l=1$ and $r=L-2-1$ as is shown in Fig. 2.

*Step 1.* An AS vector is defined and another vector (HF vector) is defined which contains the filled Hartree-Fock orbitals.

*Step 2.* Based on the ordering the AS and HF vectors are reordered and for the given partitioning the elements of the AS and HF vectors belonging to the right block are determined.

*Step 3.* The $q^3$ bases states of the $B_l\bullet\bullet$ subsystem are formed and their quantum numbers are determined.

*Step 4.* On the site given by the first element of the AS vector the basis states $(0,\uparrow,\downarrow,\uparrow\downarrow)$ are formed and the HF sites are filled according to the HF configuration except for this site if it is in the HF vector. An example is shown in Fig. 12 for the half-filled Hubbard chain using the original ordering and $M_r^{min}=8$. The quantum numbers of the obtained states are determined and those which have a matching component with any of the $B_l\bullet\bullet$ basis states satisfying the conservation of total quantum numbers are kept. Next the first two elements of the AS vector are taken and the same procedure is repeated until $M_r^{min}$ many states are selected. In this way one makes sure that states of the environment block have a matching component with the system block, thus they all produce contribution to the mutual entropy.

*Step 5.* One iteration step of the standard DMRG procedure is carried out. In the next step then procedures of steps 2–5 are repeated by forming again the $M_l\times q\times q$ states of the $B_l\bullet\bullet$ subsystem and the $M_r$ states of the right block matching the left block are determined. According to Eq. (6), in order to allow the possibility of $M_l\times q$ nonzero eigenvalues of the reduced density matrix $\rho_L$, $M_r$ is determined as $\max(M_l,M_r^{min})$.

*Step 6.* Close to the turning points it can happen that for the selected states $M_r<M_r^{min}$ thus the excluded states could never be recovered during later steps of the method. In order to avoid such a problem all $q^r$ states are selected for the environment block if $M_r<M_r^{min}$.

This procedure ensures that the size of the active space is extended dynamically as the system evolves and the left block is correlated from the very beginning with the most important states defined by the AS vector. In addition, as the size of the left and right blocks changes the second step of the procedure adjusts the AS vector so that only those elements are taken into account which belong to that given right block.

As an example, Fig. 13 shows the density-matrix spectra, the calculated mutual entropy $S$, environment block entropy $S_r$, and Kullback-Leibler entropy $K$ for three specially constructed right blocks with $M_r^{min}=64$ for the half-filled Hubbard chain with $U=1$, $L=14$ using the original ordering. In the first example we have formed the right block basis states from the sites lying close to the right-hand side of the chain as in the standard initialization procedure. The second example corresponds to a similar construction but the Hartree-Fock sites were doubly filled. In the third example the right block was set up according to the method described above. It is evident from the figure that in the first example one eigenvalue of the reduced density matrix was one giving rise to zero mutual and environment block entropies and separability of the superblock eigenstate. The second example corresponds to a finite but very small entropy while the entropy is increased for the third example. It is thus clear that a better environment block can be constructed by using the AS vector.

### B. Reducing the effective chain length during the initialization procedure

Once the $M_r$ states of the environment block are found, taking into account the conservation laws of the quantum numbers, many sites will remain unfilled as can be seen on the example shown in Fig. 12. If the right block configuration space is represented by an $M_r\times r$ matrix then those columns (sites) which contain only the empty state (labeled as E) are not active, since the action of creation and annihilation operators on such empty sites gives no matrix elements. Therefore the $i,j,k,l$ summation indices of Eq. (25) can be restricted only to the remaining nonempty sites giving rise to a much smaller effective size of the chain.

The nonempty sites fall into two further categories. Those columns (sites) which contain only doubly filled sites (D) and those called active sites (A) which contain various basis states $(0,\downarrow,\uparrow,\downarrow\uparrow)$. Several steps of the DMRG matrix algebra can be restricted to the active sites only and various restrictions are also given if an index corresponds to a doubly filled site. For example, the matrix algebra for quadratic auxiliary operators having the form $c_{i\alpha}c_{j\beta}$ with $\alpha,\beta$ corre-

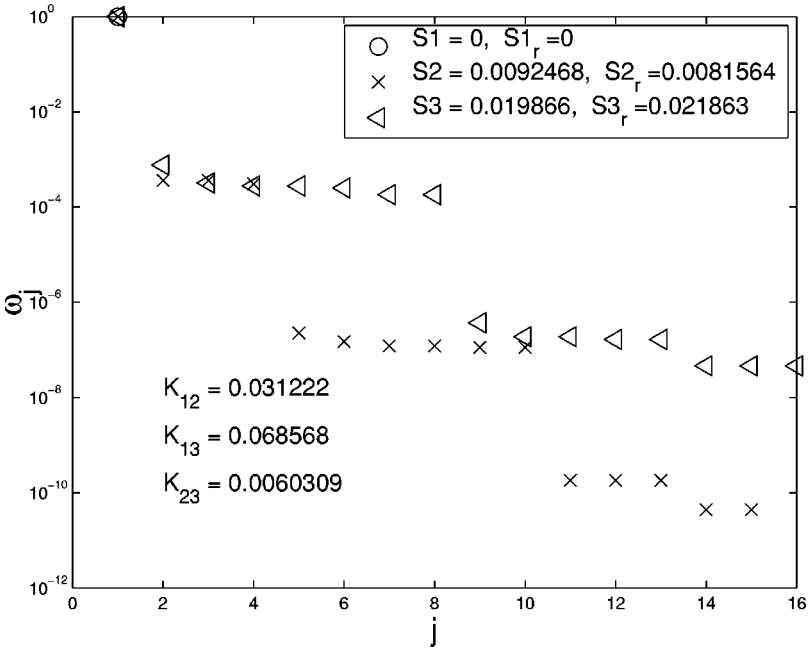


FIG. 13. The reduced density-matrix eigenvalue spectrum, the mutual von Neumann entropy $S$, environment block entropy $S_r$, and Kullback-Leibler $K$ entropy calculated for three specially constructed environment blocks for the half-filled Hubbard chain with $U=1$ and $L=14$ using the original ordering.

sponding to up or down spins, or the form $c_{i\uparrow}^{\dagger}c_{j\downarrow}$, have to be carried out only for the active sites. Therefore, the construction of auxiliary operators[3] containing various combinations of one, two, three, and four fermion operators can be obtained in a much faster way. This is especially important for the quadratic auxiliary operators since their multiplication during the diagonalization of the superblock Hamiltonian is the most time-consuming part of the MS-DMRG. It is worth mentioning that the auxiliary operators generated by the left block states have be to calculated for the empty sites as well, because during the backward sweep the structure of the right block might change and nonzero matrix elements in the superblock Hamilton operator could be generated.

This procedure has the advantage that when doubling the number of sites (doing a calculation on a larger basis set), the computational time will not increase significantly during the first half-sweep and a much larger subset of block states (larger $M_r^{min}$) can be used very efficiently to generate a better environment block. For optimal ordering this gives a much faster convergence and due to the better environment the crossover between the environment and truncation error can be reached within a few steps. After the end of the first half-sweep $M_l^{min}=M_r^{min}$ can be used.

### C. Application of Abelian point-group symmetry in QC-DMRG

When the DMRG procedure is applied in quantum chemistry to calculate the energy of molecules the use of Abelian point-group symmetry reduces the dimension of the Hilbert space to be considered. Before proceeding with the numerical results we show how to use this symmetry in QC-DMRG. The irreducible representation of each molecular orbital is generated by standard quantum chemistry programs, such as the MOLPRO program[36] package. The quantum numbers of the irreducible representations are very similar to the momentum quantum numbers $k_i$ used in MS-DMRG. The $K_i$ quantum number operator for an orbital defined on the $(0,\downarrow,\uparrow,\downarrow\uparrow)$ basis states in QC-DMRG is written as

$$K_i=k_i\begin{pmatrix}1\\0\\0\\1\end{pmatrix}+\begin{pmatrix}0\\1\\1\\0\end{pmatrix}, \tag{27}$$

where $k_i$ can take values from 1 to 8 according to the symmetry of the orbital. The symmetry quantum number operator for basis states of two orbitals is determined by using the standard character table as

$$K_{ij}=\mathcal{T}(K_i,K_j), \tag{28}$$

with

$$\mathcal{T}=\begin{pmatrix}1&2&3&4&5&6&7&8\\2&1&4&3&6&5&8&7\\3&4&1&2&7&8&5&6\\4&3&2&1&8&7&6&5\\5&6&7&8&1&2&3&4\\6&5&8&7&2&1&4&3\\7&8&5&6&3&4&1&2\\8&7&6&5&4&3&2&1\end{pmatrix}. \tag{29}$$

Using Eq. (28) we can determine the symmetry quantum numbers of all the left and right block bases states, and for a given target state we can restrict the number of electrons and the total symmetry ($K_{tot}$) as

$$K_{tot}=\mathcal{T}(K^L,K^R), \tag{30}$$

where $K_{tot}$ again can take values between 1 and 8. During the renormalization procedure, the symmetry quantum num-

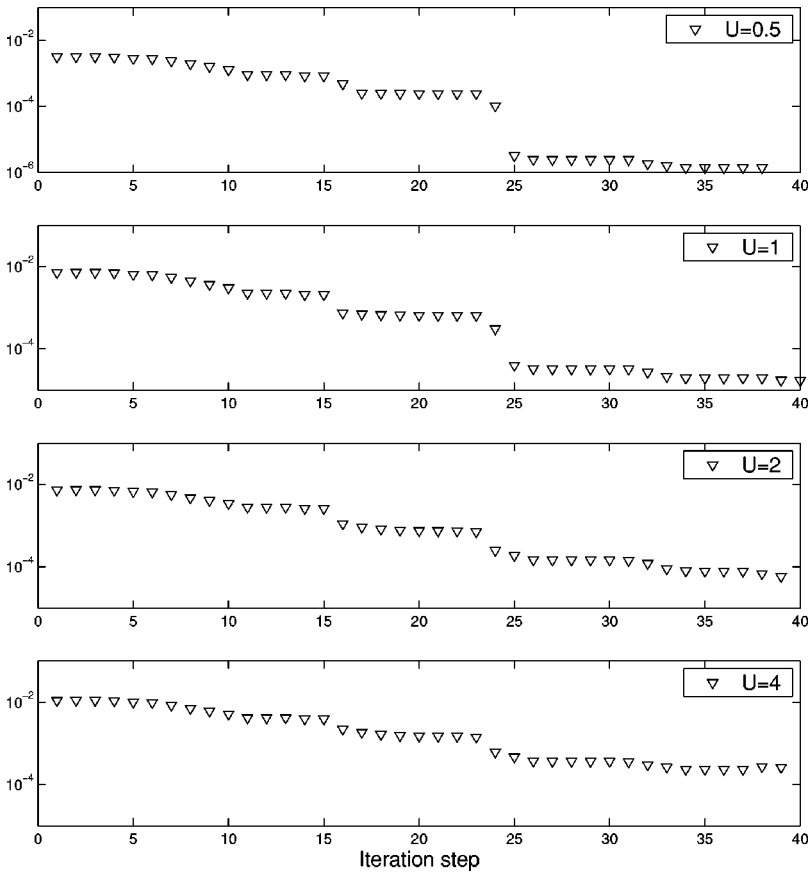


FIG. 14. The relative error as a function of iteration step for the $L=18$ half-filled Hubbard chain for $U=0.5,1,2,4$ using the DEAS procedure.

ber operators are renormalized in a similar way as the particle number operators and they are assigned to the new renormalized block states.

## VI. NUMERICAL RESULTS USING OPTIMIZED ORDERING AND DEAS

In order to demonstrate the efficiency of the DEAS procedure we have studied the 1D Hubbard chain for various fillings, orderings, $U$ values, and chain lengths. We have found that for small $U$ in the range 0.1–1 MS-DMRG converges much faster than with the ordinary initialization procedure. Performing calculations on half-filled lattices up to 30 sites the error margin set by $\mathrm{TRE}_{max}\simeq 10^{-5}$ has been reached within one and a half or two sweeps. As the strength of $U$ increased the procedure selected out more block states but the method still converged much faster. As an example, Fig. 14 shows the result obtained for the half-filled $L=18$ chain for $U=0.5,1,2,4$. In order to obtain an absolute error of $10^{-4}$, $\mathrm{TRE}_{max}$ was fixed to $10^{-5}$ and $M_{min}$ was chosen as 400 and we used the ordering shown in the sixth panel of Fig. 8. For $U=4$ we have cut the maximum number of block states at 2500 giving a maximum value of the truncation error of the order of $10^{-4}$. The AS vector is $[13,5,14,4,12,6,15,3,11,7,16,\ldots]$ and the HF vector is $[5,6,7,8,9,10,11,12,13]$. It can be seen in the figure that in all cases the desired accuracy was obtained within two sweeps in contrast to the results obtained by Nishimoto *et al.*[6] using the standard initialization procedure. It is even more important to emphasize that after the first (second) sweep the calculated momentum distribution $\langle n_k\rangle=\langle\Sigma_{i,\alpha}c^{\dagger}_{i\alpha}c_{i\alpha}\rangle$ for $U=1(U=4)$ agreed up to three digits with the values obtained by real-space DMRG with periodic boundary condition.

Similar results were found for the molecules studied. Results for the $CH_2$ molecule for fillings (number of electrons/number of orbitals) 6/13 and 6/23, $H_2O$ for 8/24, $N_2$ for 10/26, and $F_2$ for 18/18 are shown in Fig. 15. In all cases the AS vector was determined in a self-consistent way by first running a quick full sweep with some 64 block states and then it was constructed based on the decay of the site entropy values described in the preceding section. In all cases we have used the modified Cuthill-McKee ordering, according to the method described in Sec. IV. It is clear from the figure that the DMRG with the DEAS procedure converged very fast and usually 90–99 % of the correlation energy was obtained within the first one-half sweep. Therefore, the crossover between the environment and the truncation error can be reached much faster and the accuracy of the method is finally determined by $\mathrm{TRE}_{max}$ as was shown in Ref. 9. As an example for $CH_2$ for 6/13 filling the $10^{-8}$ accuracy that was shown in Fig. 6 was reached in 13 iteration steps with the DEAS procedure using the same parameter sets. For $F_2$ the $10^{-8}$ accuracy that was shown in Fig. 10 was reached in 23 iteration steps.

It is very important to mention that besides the very fast convergence, if an optimal ordering is obtained and a good initial condition is used, then the number of block states can be reduced significantly during the process of renormaliza-

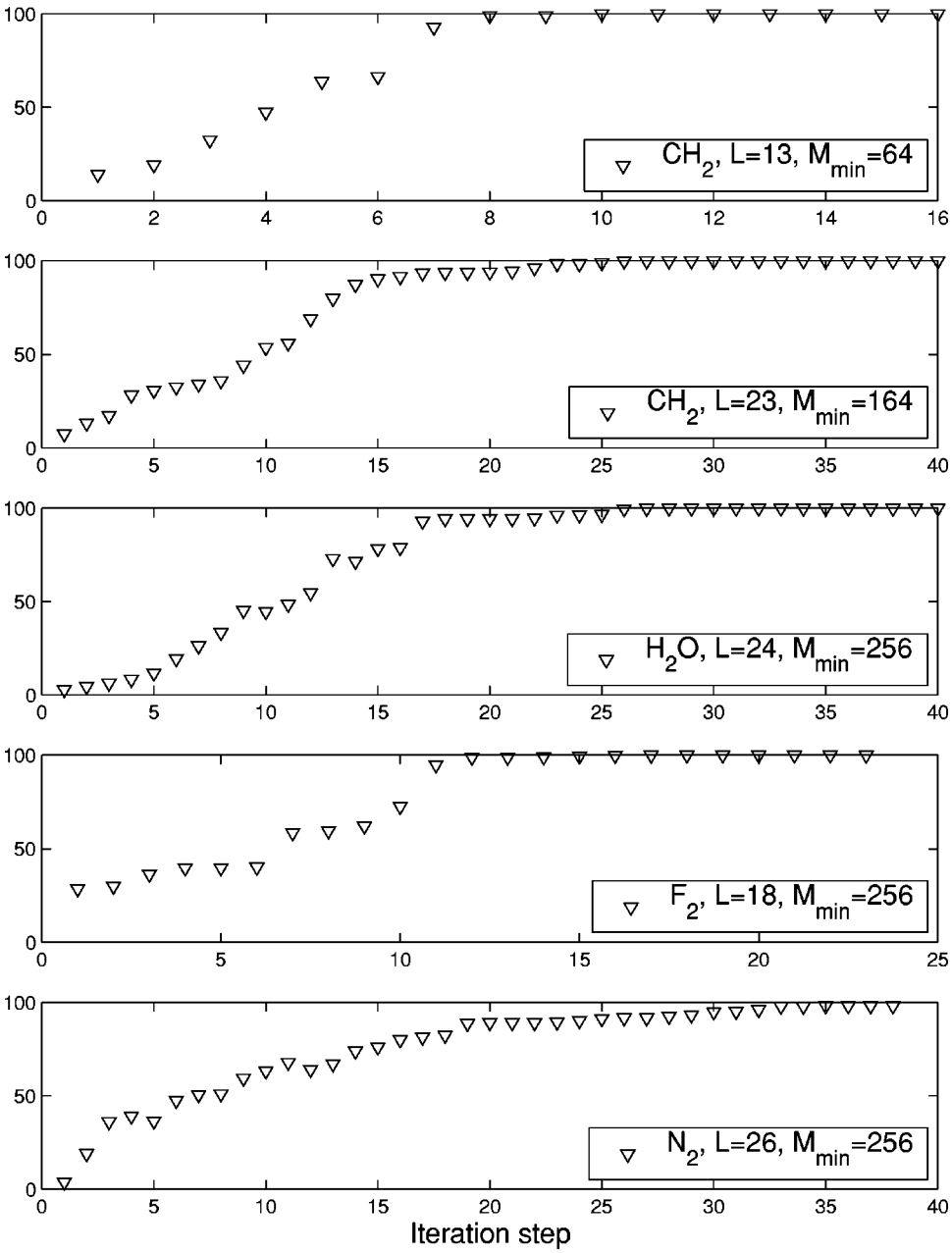


FIG. 15. Percentage of correlation energy as a function of iteration step obtained by the DEAS procedure for the $CH_2$, $H_2O$, $N_2$, $F_2$ molecules.

tion and finally a block can describe the total system very accurately. As an example we have set $M_{min}=4$ and the energy of the $CH_2$ molecule with 13 orbitals was obtained after the second sweep up to seven digit accuracy with $M_l=21$, $M_r=4$, $\dim\mathcal{G}=107$ and for $F_2$ 18/18 up to five digit accuracy with $M_l=120$, $M_r=4$, $\dim\mathcal{G}=220$ in contrast to the dimensions of the exact solution which are 230 230 and 9 075 135 300 calculated, respectively, by the $(2L)!/[(2L-N)!N!]$ formula. The same was obtained for the half-filled Hubbard model up to four digit accuracy with $L=18$, $U=1/2$ is $M_l=280$, $M_r=4$ $\dim\mathcal{G}=562$. This feature is expected to have a close relationship to quantum data compression[21,23] where the relationship between the dimension of the Hilbert space and site entropies is given as

$$\log_2(\dim\mathcal{G})=S(\otimes_i\rho_i). \tag{31}$$

Therefore, it seems to be promising to examine the separability of reduced density matrices and their effect on the number of block states. A more detailed study of the relationship between site entropies and the dimension of the Hilbert space of the superblock Hamiltonian based on Suchmacher quantum data compression is in progress.

## VII. SUMMARY AND FUTURE PROSPECTIVES

We have studied the effect of ordering of lattice sites in the momentum space version of the density-matrix renormalization-group (MS-DMRG) method by solving the 1D Hubbard chain and various molecules. This was done by calculating site and block entropies, the separability and entanglement of the target state. Our findings are listed below.

(1) We have shown that the $k_i$ sites or molecular orbitals

lying closer to the Fermi surface have larger information content and correspond to a larger mixture described by a larger von Neumann entropy and participation number.

(2) We have shown that if all the sites with large entropy are placed close to one end of the chain then this improper ordering can lead to vanishing mutual entropy, lack of entanglement and quantum information exchange between the system block and environment block. This prevents the method from converging to the target state. Therefore, the proposal by Xiang to place the highly correlated sites as close as possible is not a sufficient condition alone.

(3) If lattice sites with large entropy are moved to the two ends of the chain the block entropies can be maximized giving rise to a larger entanglement, but the convergence of the method can still be very slow or the method does not converge at all. Numerical results indicate that if these sites are moved to the center of the chain, then a very fast convergence can be obtained with a much smaller subset of block states. We have found that the mutual entropy has sharp peaks when the most active sites are just between the system and environment blocks when the energy also improves significantly. Furthermore, in order to have a finite interaction between the blocks some sites with smaller but finite entropies have to be placed close to the ends of the chain. This keeps the block entropy above a critical value for several iteration steps. We have shown that these conditions are often not satisfied when using the Cuthill-McKee algorithm.

(4) We have developed an initialization procedure which gives finite block entropies even during the first half-sweep of MS-DMRG and reduces the volume of separable basis states of the target state. This method extends the active space in a dynamical fashion resulting in a very accurate set of renormalized block states and a very fast convergence. For the models that have been studied 90–99 % of the correlation energy was obtained within the first half-sweep.

(5) We have shown that MS-DMRG is very sensitive to the ordering and the initial conditions. A good starting configuration and an optimized ordering can result in very accurate blocks with very limited number of block states which still describes the system with the accuracy determined in advance.

We expect that DMRG can be a very good candidate for a new method on quantum data compression and on quantum error correction[27,38,39] in which case the fidelity can be defined in advance by $\mathrm{TRE}_{max}$. This research is in progress.

Since MS-DMRG describes a composite system with long-range interactions it is expected that the method could be used in the context of nonextensive thermodynamics to study models for which the subadditivity of the subsystem entropy does not hold. This would allow one to investigate Tsallis entropy,[40] nonextensive mutual entropy, and quantum entanglement by using the generalized Kullback-Leibler entropy.[41]

## ACKNOWLEDGMENTS

This research was supported in part by the Fonds der Chemischen Industrie and the Hungarian Research Fund(OTKA) Grant Nos. 30173, 32231, and 43330. Ö.L. acknowledges useful discussions with B.A. Hess and G. Fáth. The authors also thank Holger Benthien for providing results for the Fermi momentum distribution curve obtained with real-space DMRG using periodic boundary conditions.

[1] S.R. White, Phys. Rev. Lett. **69**, 2863 (1992).
[2] S.R. White, Phys. Rev. B **48**, 10345 (1993).
[3] T. Xiang, Phys. Rev. B **53**, 10445 (1996).
[4] S.R. White and R.L. Martin, J. Chem. Phys. **110**, 4127 (1998).
[5] S. Daul, I. Ciofini, C. Daul, and S.R. White, Int. J. Quantum Chem. **79**, 331 (2000).
[6] S. Nishimoto, E. Jeckelmann, F. Gebhard, and R.M. Noack, Phys. Rev. B **65**, 165114 (2002).
[7] A.O. Mitrushenkov, G. Fano, F. Ortolani, R. Linguerri, and P. Palmieri, J. Chem. Phys. **115**, 6815 (2001).
[8] G.K.-L. Chan and M. Head-Gordon, J. Chem. Phys. **116**, 4462 (2002).
[9] Ö. Legeza, J. Röder, and B.A. Hess, Phys. Rev. B **67**, 125114 (2003).
[10] Ö. Legeza, J. Röder, and B.A. Hess, Mol. Phys. **101**, 2019 (2003).
[11] H. Barnum, C.M. Caves, C.A. Fuchs, R. Jozsa, and B.W. Schumacher, Phys. Rev. A **54**, 4707 (1996).
[12] M. Horodecki, P. Horodecki, and R. Horodecki, Phys. Rev. Lett. **80**, 5239 (1998).
[13] M. Horodecki and P. Horodecki, Phys. Rev. A **59**, 1799 (1998).
[14] K. Zyczkowski, P. Horodecki, A. Sanpera, and M. Lewenstein, Phys. Rev. A **58**, 883 (1998).
[15] G. Vidal and R. Tarrach, Phys. Rev. A **59**, 141 (1999).
[16] G. Vidal and R.F. Werner, Phys. Rev. A **65**, 032314 (1999).
[17] S.L. Braunstein, C.M. Caves, R. Jozsa, N. Linden, S. Popescu, and R. Schack, Phys. Rev. Lett. **83**, 1054 (1999).
[18] R. Jozsa and J. Schlienz, Phys. Rev. A **62**, 012301 (2000).
[19] H. Barnum, Phys. Rev. A **62**, 042309 (2000).
[20] C.W. Bauschlicher, Jr., and S. Langhoff, J. Chem. Phys. **89**, 4246 (1988).
[21] R. Jozsa, J. Mod. Opt. **41**, 2315 (1994).
[22] R. Jozsa and B. Schumacher, J. Mod. Opt. **41**, 2343 (1994).
[23] B. Schumacher, Phys. Rev. A **51**, 2738 (1995).
[24] R. Jozsa, M. Horodecki, P. Horodecki, and R. Horodecki, Phys. Rev. Lett. **81**, 1714 (1998).
[25] A. Peres, Phys. Rev. Lett. **77**, 1413 (1996).
[26] M. Horodecki, P. Horodecki, and R. Horodecki, Phys. Lett. A **223**, 8 (1996).
[27] C.H. Bennett, D.P. DiVicenzo, J.A. Smolin, and W.K. Wootters, Phys. Rev. A **54**, 3824 (1996).
[28] W.K. Wootters, Phys. Rev. Lett. **80**, 2245 (1998).
[29] V. Vedral and M.B. Plenio, Phys. Rev. A **57**, 1619 (1998).
[30] C.H. Bennett, H.J. Bernstein, S.P. Popescu, and B. Schumacher, Phys. Rev. A **53**, 2046 (1996).
[31] M. Lewenstein and A. Sanpera, Phys. Rev. Lett. **80**, 2261 (1998).
[32] E. Shannon, Bell Syst. Tech. J. **27**, 379 (1948).
[33] H. Haken, *Information and Self-Organization* (Springer, Berlin, 2000).

[34] S. Kullback and R.A. Leibler, Ann. Math. Stat. **22**, 79 (1951).
[35] S. Kullback, *Information Theory and Statistics* (Wiley, New York, 1959).
[36] R. D. Amos, A. Bernhardsson, A. Berning, P. Celani, D. L. Cooper, M. J. O. Deegan, A. J. Dobbyn, F. Eckert, C. Hampel, G. Hetzer, P. J. Knowles, T. Korona, R. Lindh, A. W. Lloyd, S. J. McNicholas, F. R. Manby, W. Meyer, M. E. Mura, A. Nicklass, P. Palmieri, R. Pitzer, G. Rauhut, M. Schütz, U. Schumann, H. Stoll, A. J. Stone, R. Tarroni, T. Thorsteinsson, H.-J. Werner (unpublished), MOLPRO, a package of ab initio programs designed by H.-J. Werner and P. J. Knowles, version 2002. 1, 2002.
[37] E. Cuthill and J. McKee (unpublished).
[38] P.W. Shor, Phys. Rev. A **52**, R2493 (1995).
[39] I.L. Chuang and Y. Yamamoto, Phys. Rev. Lett. **76**, 4281 (1996).
[40] C. Tsallis, J. Stat. Phys. **479**, 479 (1988).
[41] S. Abe, Phys. Rev. A **60**, 3461 (1999).